*Journal of Ceramic Processing Research. Vol. 13, Special. 1, pp. s16~s21 (2012)*

J O U R N A L O F
**Ceramic Processing Research**

# Magnetron sputtering of TiAlN films for inkjet printhead resistors

**Sang Min Ha, Min Ho Park and Sang Ho Kim***
*Department of Materials Engineering, Korea University of Technology and Education, 1800 Chungjeol-ro, Byungcheon-myun, Dongnam-gu, Cheonan, Chungnam 330-708, Korea*

**Heat resistors in thermal inkjet printheads require a low temperature coefficient of resistance (TCR) and good oxidation resistance. Titanium aluminum nitride (TiAlN) films, which have a lower TCR and better oxidation resistance than the conventional TaN and TaAl films, were deposited on a Si(100) substrate at 400 °C by radio frequency (RF) magnetron co-sputtering using TiN and AlN ceramic targets. This study investigates the effect of $N_2$ flow rates on the TCR and the oxidation resistance of the TiAlN films. The best TCR value was -390.35 ppm/k and the lowest sheet resistivity change was 31%. These results were obtained with high a $N_2$ flowing of 10%, and discussed from the microstructural and stoichiometric viewpoints. The grain-size and surface-roughness decreased with the increasing $N_2$ flow rate, thus resulting in small grains. When the $N_2$ flow rate was as high as 10%, the Ti 2p, Al 2p, and N 1s orbital electron binding energies from XPS analyses showed that the nitrogen content in the TiAlN films exceeded the stoichiometry. The small grains and excess nitrogen made the film's sheet resistance higher, within a relevant range, and provided low TCR and high oxidation resistance.**

**Key words : Magnetron sputtering, TiAlN, Heat resistor, Temperature coefficient of resistance (TCR), Inkjet printhead.**

## Introduction

The drop-on-demand (DOD) inkjet printing method has a slower printing speed, but its usage is increasing due to its low electricity levels, less ink consumption, and simple production process [1]. Heat resistor films are the most important part of inkjet printheads because they must have a low temperature coefficient of resistance (TCR) for stable ink ejection and a strong resistance against both corrosion and oxidation to prevent degradation.

Titanium aluminum nitride (TiAlN) was developed as a promising alternative to binary coating materials for cutting and forming tools [2, 3]. However, its level of resistivity is in a suitable range for resistor films. Furthermore, they contain Al, which is expected to have superior properties for a good oxidation resistance [4]. They are also extremely hard, have super wear-resistance, lower thermal expansion, and enhanced erosion-resistance compared to commercial TaN resistors [5], which make it a suitable material for inkjet resistor films where a high operation temperature, chemical attacks by the ink, and mechanical stresses from cavitation forces arise [6].

The TCR value of commercial $TaN_{0.8}$ is 336 ppm/k [7]. In addition to the advantages of TiAlN films, a comparable TCR is inevitable. Therefore, the effect of the $N_2$ flow rate on the TCR and oxidation resistance of the films was investigated by relating them to micro morphology and stoichiometry.

*Corresponding author:
Tel : +82-41-560-1325
Fax: +82-41-560-1360
E-mail: shkim@koreatech.ac.kr

## Experimental

TiAlN films approximately 200 nm thick were deposited on the Si(100) substrate by radio-frequency magnetron sputtering (SVSP-3M3-500 model) using stoichiometric TiN (99.99%) and AlN (99.99%) targets under various $N_2$ flow rates. Prior to loading them to the chamber, Si(100) substrates were cleaned ultrasonically in ethanol and deionized water for 20 minutes. Fig. 1 illustrates the deposition system used in this study; Deposition chamber was evacuated to $8\times10^5$ Pa ($=6\times10^7$ torr) prior

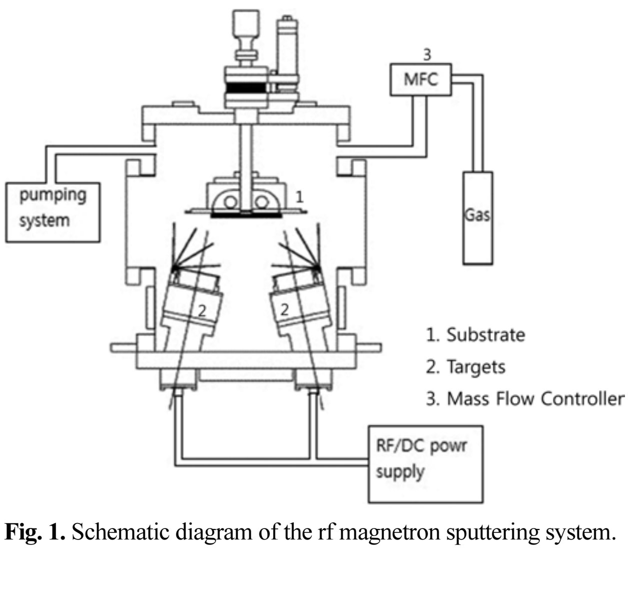


**Fig. 1.** Schematic diagram of the rf magnetron sputtering system.

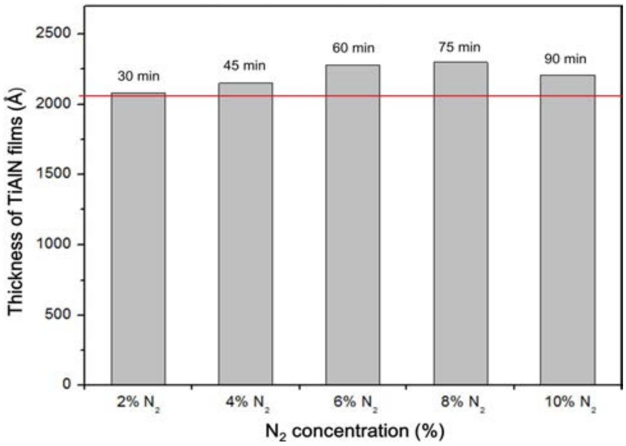


**Fig. 2.** Thickness of TiAlN films deposited at the different $N_2$ ratios.

**Table1.** Sputtering conditions of TiAlN films

| Parameters | Values |
|---|---|
| Base pressure (Pa) | < $6\times10^{-7}$ Torr |
| Sputtering pressure (Torr) | $5\times10^{-3}$ Torr |
| Distance of cathode to substrate (mm) | 100 |
| Target (2 inches in diameter) | TiN(99.99%), AlN(99.99%) |
| RF Power (TiN) | 200 W |
| RF Power (AlN) | 300 W |
| Substrate temperature (°C) | 400°C |
| Rotational speed of the substrate (rpm) | 4 rpm |
| Deposition time (min) | 30~90 min |
| Total flow rate | 30sccm |

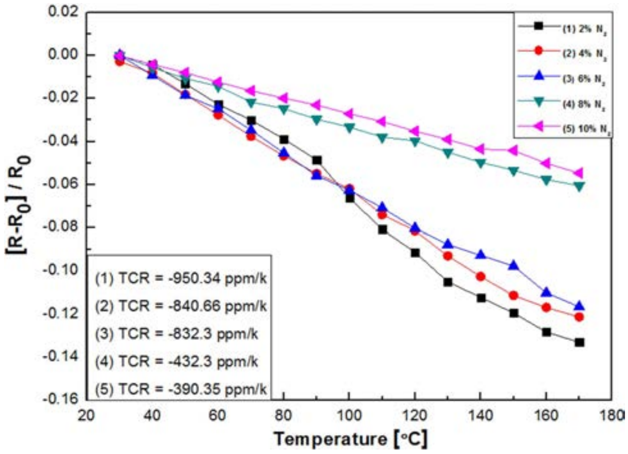


**Fig. 3.** TCR of TiAlN films deposited at the different $N_2$ ratios.

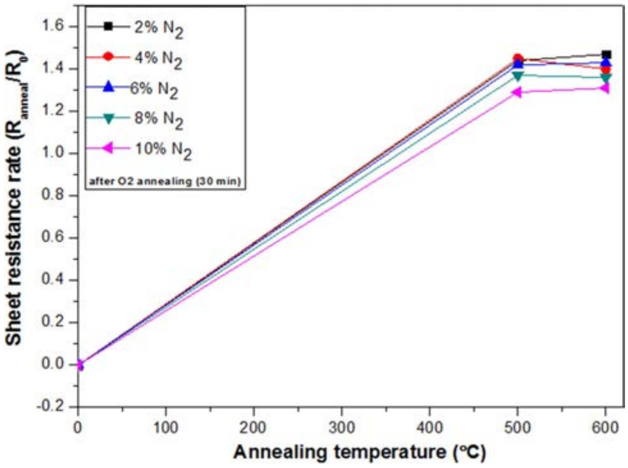


**Fig. 4.** Oxidation resistance measured by sheet resistance change of TiAlN films deposited at the different $N_2$ ratios.

to deposition. The flow rate of each gas ($N_2$ and Ar) was controlled independently using mass flow controllers (MFC) to make the flow rate of the $N_2$ reach 2 to 10% and to maintain the total flow rate constant of 30 sccm. In order to avoid target contamination and precisely control the nitride formation, the nitrogen flow rate was reduced from high to low. While it maintained its thickness, which was measured by α-step (TENCOR-2) at approximately 2000 Å by adjusting the deposition time (Fig. 2), the $N_2$ flow rate varied in accordance with the other fixed deposition parameters in the conditions shown in Table 1.

The film's concentrations of Al and Ti (at. %) were analyzed using energy dispersive spectroscopy (EDS), and the ratio varied within a small range near 1:1. The preferred growth orientation and crystallinity were characterized by X-ray diffraction (XRD, Rigaku RTP 200RC) in the 2θ range of 20~70° with Cu Kα radiation. The surface morphology of the films was observed using atom force microscopy (AFM, Solver P47-PRO) and field emission scanning electron microscopy (FESEM, JEOL JEM-7500F). The chemical state of the films was analyzed using X-ray photoelectron spectroscopy (XPS, Sigma Probe -ThermoVG, U.K) with Al Kα radiation, and the peaks were calibrated by employing the C 1s peak at 284.6 eV. The TCR was measured by a digital multimeter (HP3457A) while heating the films from 30 to 170 °C in a thermostatically controlled oven. The oxidation resistance inferred from the sheet resistance changes was measured using a four-point probe (Guardian scientific 402S) after maintaining 500 and 600 °C for 30 minutes.

## Results and discussion

Fig. 3 indicates the TCR value of the films calculated using the following formula, TCR (ppm/k) = $(R_{170} - R_{30})/[R_{30}(170\text{-}30)]\times10^6$ with the different $N_2$ flow rates. The low TCR value of heat resistors in inkjet printheads is favorable for the reliability of constant ink injection. TCR value of our sample is -390.35 ppm/k at 10% $N_2$, which is a good result compared with that of commercially used $TaN_{0.8}$ (-336 ppm/k) [7]. The TCR

**Table 2.** Sheet resistance change of TiAlN films deposited at the different $N_2$ ratio (Units: Ω/ □ )

| | Before | After (600°C, 30 min) | Change |
|---|---|---|---|
| 2% $N_2$ | 191.88 | 282.25 | 47% |
| 4% $N_2$ | 180.01 | 252.93 | 40% |
| 6% $N_2$ | 232.35 | 333.6 | 43% |
| 8% $N_2$ | 284.02 | 385.76 | 36% |
| 10% $N_2$ | 286.46 | 375.92 | 31% |

increased with a lower $N_2$ flow rate, particularly from the 8% to 6% $N_2$. Between these two points, the transition point where N saturation in TiAlN and N interstitials by excess N atoms is thought occur; later XPS analyses will confirm and discuss this.

Fig. 4 indicates the sheet resistance inferred the oxidation resistance of TiAlN film, which was already considered an excellent oxidation resistant material [8], was varied via annealing at 600 °C from 31 to 47% according to the $N_2$ ratio (Table 2). It was widely reported that the oxidation behavior of TiAlN is controlled by Al content [9], which forms an amorphous $Al_2O_3$ at the surface layer and makes oxygen diffusion through the film difficult. However, since the films in this study were controlled to have a similar Al content, the oxidation resistance variation is expected to result from other factors such as dense morphology and high N interstitials, which makes it difficult for the oxygen to diffuse into the grains.

Fig. 5 demonstrates the sheet resistance variation with the $N_2$ flow rate. The sheet resistance increased with the $N_2$ flow rate, particularly between 4% and 8% $N_2$. This is similar to the previously explained TCR change, therefore it appears that an important transition

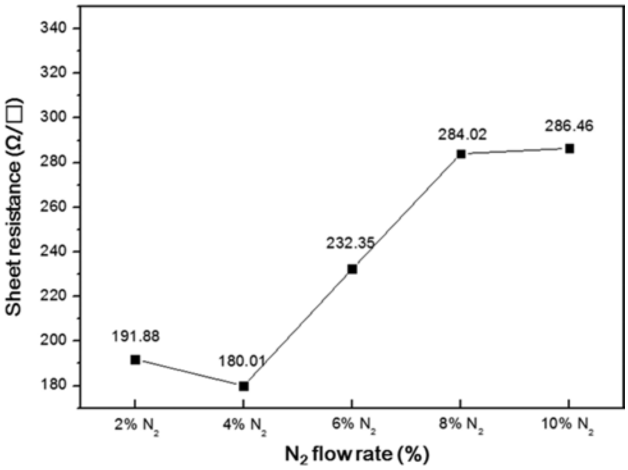


**Fig. 5.** Sheet resistance of TiAlN films deposited at the different $N_2$ ratios.

occurs within this range. The TCR for conductive metals is within a few thousand ppm/k and conductive ceramics are within a few hundred ppm/k that decrease with high resistance. High sheet resistance, if it is in a compromising electricity consumption range, can be the main reason of better TCR at a high $N_2$ ratio.

Fig. 6 and Fig. 7 show the surface morphology and roughness of the TiAlN films. The surface morphology presents smaller grains with a higher $N_2$ ratio-approximately 100 nm grains with 2 and 4% $N_2$, 50 nm grains with 6% $N_2$ , 30 nm grains with 8% $N_2$, and smaller than 15 nm grains with 10% $N_2$, respectively. This is similar to the morphologies reported for TiN with $N_2$ variations by Chakrabarti et al. [10] and Hones et al. [11]. Morphology differences significantly influence the resistance and oxidation behavior of the films since electrons and oxygen molecules use the same path

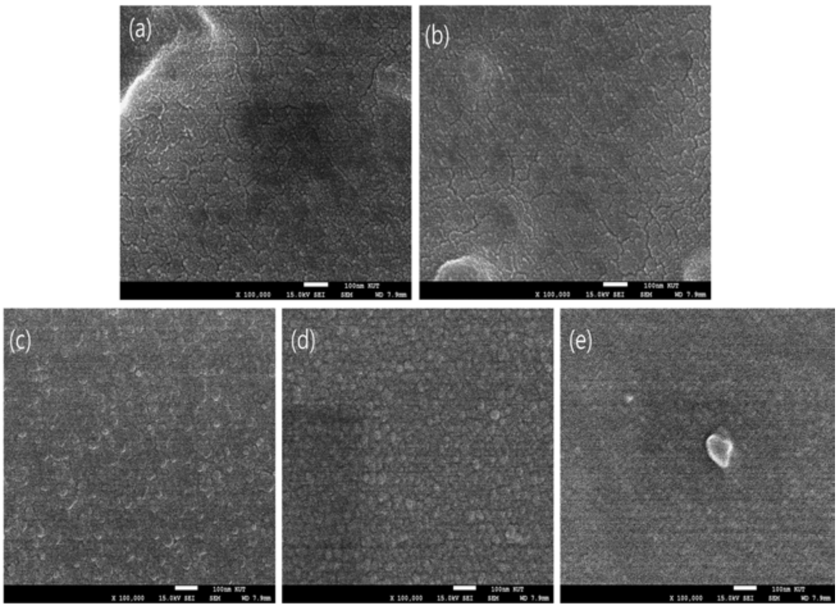


**Fig. 6.** FESEM photograph of TiAlN films deposited at the different $N_2$ ratios; (a) 2%, (b) 4%, (c) 6%, (d) 8%, and (e) 10%.

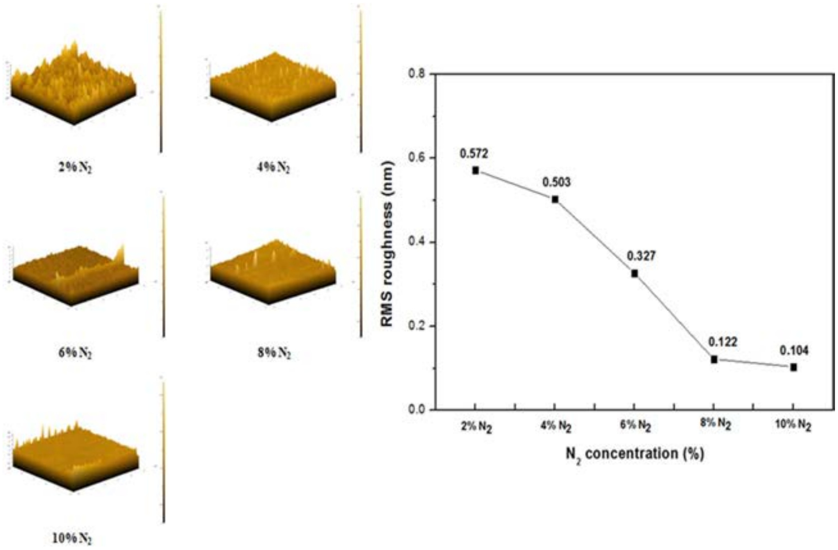


**Fig. 7.** AFM surface morphologies of TiAlN films deposited at the different $N_2$ ratios.

through the grain boundaries [12]. Most conductive materials change their specific resistance in different temperatures. This is why the values of resistances are always specified at a standard temperature (usually 20 or 25 °C). According to the von Glasow [13], the resistivity, ρ, of a metal film can be divided into two terms : $\rho = \rho_T(T)+\rho_R$, where $\rho_T$ is a temperature-dependent component that is attributed to electron scattering at phonons and $\rho_R$ is a temperature-independent term arising from electron scattering at lattice imperfections (e.g. surfaces, grain boundaries, defects, impurities). In a temperature range where ρ is proportional to T, the TCR of a crystalline material is defined by:

$$TCR = \frac{R_1 - R_2}{R_t(T_1 - T_2)} \tag{1}$$

where $R_1$ and $R_2$ are resistances at the temperatures $T_1$ and $T_2$, respectively and $R_t$ is resistance at a reference temperature. Since the absolute resistance, R, is proportional to resistivity, ρ, the TCR can also be expressed by:

$$TCR = \frac{\rho_T(T_1) - \rho_T(T_2)}{(\rho_T(T) + \rho_R)(T_1 - T_2)} \tag{2}$$

This equation shows that the TCR is also dependent on differences in the residual resistivity, $\rho_R$, which is the result of different microstructures. For example, the TCR value will decrease with increasing $\rho_R$ because of reduced grain size or increasing numbers of impurities or crystal defects [13]. We obtained a low TCR value of -390.35 ppm/k at a 10% high $N_2$ flow rate with small grains and $N_2$ interstitials on the films. Hones et al. proved that the morphology of TiN significantly affects the oxidation rate, and films with a pronounced columnar morphology oxidized faster than those with dense and fine-grained morphology did [11]. At higher $N_2$ flow rates, TiAlN films that have the same B1-NaCl lattice structure with TiN in less than 60% Al content [14] showed a finer and denser morphology, which resulted in better oxidation resistance. The AFM surface morphology and roughness of TiAlN films shown in Fig .7 confirms the finer grains observed in the previous FESEM images. The roughness decreased with making fine grains as the $N_2$ flow increased. This could also be affected by the presence of N interstitials that interrupt grain growth [15], and is comparable to the second phase of $Cr_2N$ in CrN film growth [12] in a high $N_2$ ratio, which leads to a smoother surface.

Fig. 8 shows the XRD pattern of the TiAlN films prepared with different $N_2$ ratios. Relatively intense (111) and (220) preferred growth orientations are seen [16]. It is also seen that when the $N_2$ ratio increases, the peak intensity decreases and the full width at half maximum (FWHM) increases. According to Shew et al. [17], the high flow rate of $N_2$ reduces the (111) peak

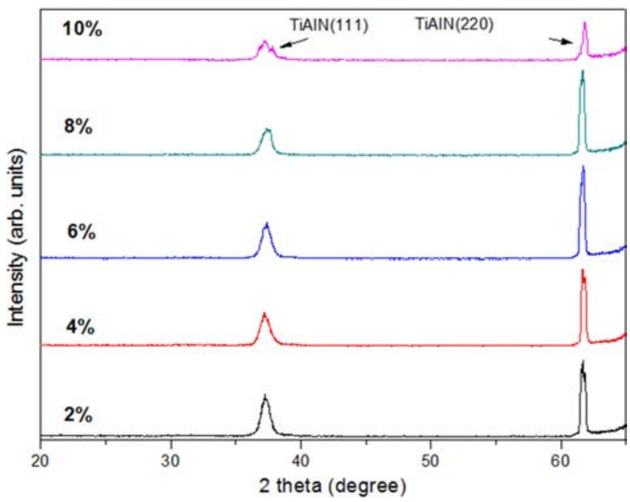


**Fig. 8.** XRD patterns of TiAlN films deposited at different $N_2$ ratios.

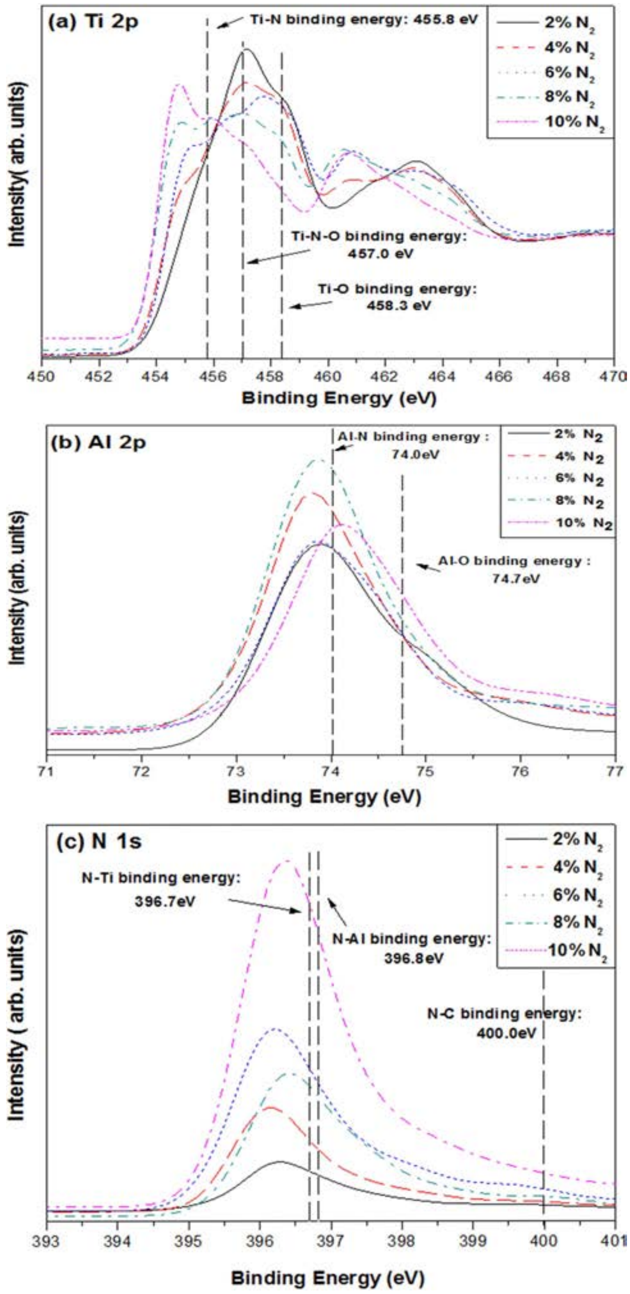


**Fig. 9.** XPS analysis of TiAlN films deposited at the different $N_2$ ratios.

because the (111) plane, with the lowest surface energy in the B1-NaCl TiAlN structure, provides favorable stacking areas for mobile atoms, which results in the lowest energy crystal facets parallel to the substrate under relatively intense bombardment. The (220) peaks also tend to decrease during the same process. The low peak intensity and bigger FWHM at a high $N_2$ ratio means that the films have low crystallinity and small grains.

Fig. 9 demonstrates the XPS analysis of the TiAlN films. The binding states of the Ti 2p spectra shown in Fig. 9(a) consist of three peaks that correspond to Ti $2p_{3/2}$ from 450 to 462 eV centered at 455.8 (Ti-N), 457 (Ti-N-O) and 458.3 (Ti-O) eV [18]. With 2%, 4%, and 6% $N_2$, the Ti $2p_{3/2}$ peak shoulders are higher on the high binding energy assigned to Ti-N-O and Ti-O. However, with 8 and 10% $N_2$, the peak shoulders are higher at the low binding energy of Ti-N bonds. When the $N_2$ flow is low, the N sites connected to the Ti atoms in the TiAlN with a B1-NaCl lattice structure are empty in some places. By incorporating more N atoms at higher $N_2$ flowing, the lattice N sites will be firstly occupied and then interstitial N atoms will remain between them. Therefore, the excess N atoms will move the Ti peaks from high to low binding energy. On the other hand, Al atoms, having a strong affinity with N atoms, kept the peak position constant for the near low binding energy of Al-N in the N deficit condition; however, with the introduction of extra N, the peaks moved to high binding energy by adding the interstitial N effect as shown in Fig. 9(b). The N atoms, attracted by Al atoms preferably at the low N concentration, were shifted to Ti atoms by increasing the concentration between 4% and 6%, which moved the N 1s peak position in the Ti-N direction. Increasing $N_2$ further creates the interstitials N effect that moves the N 1s peak to the high binding side. The position of the N 1s peaks can be identified in Fig. 9 (C).

## Conclusion

TiAlN films were deposited by rf magnetron sputtering as a function of $N_2$ flow rate. TCR and oxidation resistance, which are major requirements for inkjet printheads, were investigated in this study.

(1) With a high of 10% $N_2$ flowing, the low TCR value of -390.35 ppm/k and high oxidation resistance with a low change of sheet resistance of 131% were obtained.

(2) The low TCR and high oxidation resistance at the high $N_2$ flow rate were ascribed to the relevantly high sheet resistance due to the small grains and N interstitials.

(3) The TCR of TiAlN with 10% $N_2$ flowing was -390.35 ppm/k, which is comparable to the 336 ppm/k of commercial $TaN_{0.8}$. In addition, TiAlN has many advantages in terms of oxidation, wear resistance, and chemical inertness.

## Acknowledgements

This work was supported by a grant from the Fundamental R&D program for Core Technology of Materials funded by the Ministry of Knowledge Economy, Republic of Korea, and Educational research fund of Korea University of Technology.

## References

1. L. Kuhn and R.A. Myers, "Scientific American", Vol. 240, no.4, 120(1979)

2. W.D. Munz, J. Vac. Sci. Techol. A 4 (1986) 2717.
3. S.K. Wu, H.C. Lin, D.L. Liu, Surf. Coat. Technol. 124 (2000).
4. J.G Han, J.S. Yoon, H.J. Kim, K. Song, Surf. Coat. Technol. 86-87 (1996) 82-87.
5. T.H. Cha, D.G. Park, T.K. Kim, S.A. Jang, I.S, Yeo, J.S. Roh, J.W. Park, Appl. Phys. Letter 81 (2002) 4192-4194.
6. Q. Yang, D.Y. Seo, L.R. Zhao, X.T. Zeng, Surf. Coat. Technol. (2004) 188-189.
7. S.H. Kwon, S.W. Kang, K.H. Kim, Applied Physics Letters, 2008, 92: 181903
8. J.H. Hsieh, C. Liang, C.H. Yu, W. Wu, Surf. Coat. Technol.108y109 (1998) 132.
9. D. McIntyre, J.E. Greene, G. Hakansson, J.E. Sundgren, W.D. Munz. J. Appl. Phys. 67 (1990)1542.
10. K. Chakrabarti, J.J. Jeong, S.K. Hwang, Y.C. Yoo, C.M. Lee, Thin Solid Films 406 (2002)159-163.
11. P. Hones, C. Zakri, P.E. Shmid, F. Levy, O.R. Shojael, Appl.Phys. Lett. 76 (2000) 3194.
12. K. Chakrabarti, J.J. Jeong, S.K. Hwang, Y.C. Yoo, C.M. Lee., Thin. Solid. Films 406 (2002) 159-163.
13. A. von Glasow, IEEE 03CH37400. 41st Annual International Reliability Physics Symposium.
14. Ayako Kimura,Masahiro Kawate, Hiroyuki Hasegawa, Tetsuya Suzuki, Surf.Coat.Technol.169-170 (2003) 367-370.
15. Z.B. Zhao, Z.U. Rek, S.M. Yalisove and J.C. Bilello. Thin Solid Films, **472** (2005) 96-104.
16. C.W. Kim, K.H. Kim, Thin Solid Films 307 (1997) 113-119.
17. B.Y. Shew, J.L. Huang, D.F. Lii, Thin Solid Films 293 (1997) 212.
18. J. Sjölén, L. Karlsson, S. Braun, R. Murdey, A. Hörling and L. Hultman. Surf. Coat. Technol., **201** (2007) 6392-6403.
19. D.-Y. Wang, Y.-W. Li, C.-L. Chang and W.-Y. Ho. Surf. Coat. Technol., **114** (1999) 109-113.